doi:10.1006/jmbi.2001.4536 available online at http://www.idealibrary.com on IDEAL® *J. Mol. Biol.* (2001) **307**, 1103–1112

JMB

The Importance of Hinge Sequence for Loop Function and Catalytic Activity in the Reaction Catalyzed by Triosephosphate Isomerase

Jingyi Xiang, Jeonghoon Sun and Nicole S. Sampson*

Department of Chemistry, State University of New York, Stony Brook, NY 11794-3400, USA

**Corresponding author*

We have determined the sequence requirements for the N-terminal protein hinge of the active-site lid of triosephosphate isomerase. The codons for the hinge (PVW) were replaced with a genetic library of all possible 8000 amino acid combinations. The most active of these 8000 mutants were selected using *in vivo* complementation of a triosephosphate isomerase-deficient strain of *Escherichia coli*, DF502. Approximately 0.3 % of the mutants complement DF502 with an activity that is between 10 and 70 % of wild-type activity. They all contain Pro at the first position. Furthermore, the sequences of these hinge mutants reveal that hydrophobic packing is very important for efficient formation of the enediol intermediate. However, the reduced catalytic activities observed are not due to increased rates of loop opening. To explore the relationship between the N-terminal and C-terminal hinges, three semi-active mutants from the N-terminal hinge selection experiment (PLH, PHS and PTF), and six active C-terminal hinge mutants from previous work (NSS, LWA, YSL, KTK, NPN, KVA) were combined to form 18 ''double-hinge'' mutants. The activities of these mutants suggest that the N-terminal and C-terminal hinge structures affect one another. It appears that specific side-chain interactions are important for forming a catalytically active enzyme, but not for preventing release of the unstable enediol intermediate from the active site of the enzyme. The independence of intermediate release on amino acid sequence is consistent with the absence of a ''universal'' hinge sequence in structurally related enzymes.

Keywords: lid; loop; hinge; *in vivo* complementation; α/β barrel

Introduction

To carry out their precise functions, proteins have an intrinsic flexibility that allows different segments to move in relation to one another with relatively small energy consumption.[1-3] One catalytic device that allows a wide range of segmental motions is a protein hinge. A protein hinge is characterized by conformational changes localized to the hinge with the variation occurring in a few main-chain torsion angles. Thus, hinges can efficiently allow large domain displacements as well as movements of smaller fragments such as Ω loops.

The Ω loops are present on the surfaces of enzymes. In some cases, they form active-site lids on the surface of a protein and play a critical role for efficient catalysis. One such hinged lid is the active-site Ω loop of triosephosphate isomerase (TIM), loop 6. This loop is located between β-strand 6 and α-helix 6. The loop is conserved in other α/β TIM barrel proteins such as the α-subunit of tryptophan synthase (residues 177-191),[4,5] ribulose bisphosphate carboxylase,[6] and *Yersinia* protein tyrosine phosphatase.[7-9] As shown

J. Xiang and J. Sun contributed equally to this work.

Present address: J. Sun, Department of Pharmaceutical Chemistry, 513 Parnassus Avenue, University of California, San Francisco, CA 94143-0446, USA.

Abbreviations used: TIM, triosephosphate isomerase; WT, wild-type; DHAP, dihydroxyacetone phosphate; GAP, (*R*)-glyceraldehyde-3-phosphate; PGH, phosphoglycolohydroxamate; 2-PGA, 2-phospho-D-glycerate; GOPDH, α-glycerol-3-phosphate dehydrogenase; DEAE, diethylaminoethyl; TEA, triethanolamine; TBE, tris-borate/EDTA; FPLC, fast protein liquid chromatography; CIP, calf intestinal alkaline phosphatase.

E-mail address of the corresponding author: nicole.sampson@sunysb.edu

0022-2836/01/041103–10 $35.00/0

in Figure 1, large-scale Ω loop displacements, about 7 to 10 Å at the tip with pivoting at the hinges, are detected by X-ray crystallography. As a prototypical α/β barrel enzyme and as an intensively well characterized enzyme, TIM is an excellent model system for the study of protein hinges. Here, we describe our experiments to elucidate the structural requirements for a pair of protein hinges.

Loop 6, the active-site lid of TIM, is composed of 11 amino acid residues, and is believed to open and close as a rigid lid.[10-12] In this loop, there is a three residue N-terminal hinge (residues 166-168), a five residue hydrophobic lid (169-173), and a three residue C-terminal hinge (174-176) (Figure 2). Previously, we determined the three residue sequences that would function at the C-terminal hinge of TIM.[13] These sequences were determined using a combinatorial library and *in vivo* complementation of a TIM-deficient *Escherichia coli* strain. We found that, in addition to the expected wild-type-like sequences, three new families of three residue sequences could function as hinges. In particular, pairs at the second (175) and third (176) positions were strongly conserved. We hypothesized at that time that the absence of these three families in the more than 81 known TIM sequences indicated that not all of sequence space is accessible during evolution.

Here, we describe the application of our previously developed library methodology to the N-terminal hinge of TIM. The N-terminal hinge begins just after the active-site residue Glu165 and is heavily conserved throughout evolution (Figure 3). Its conservation suggested that the active sequences would be much more limited than that of the C-terminal hinge. We performed selections on two libraries. We first examined the sequence-dependence of the N-terminal hinge alone. Then we considered the interdependence of sequences at the two hinges.

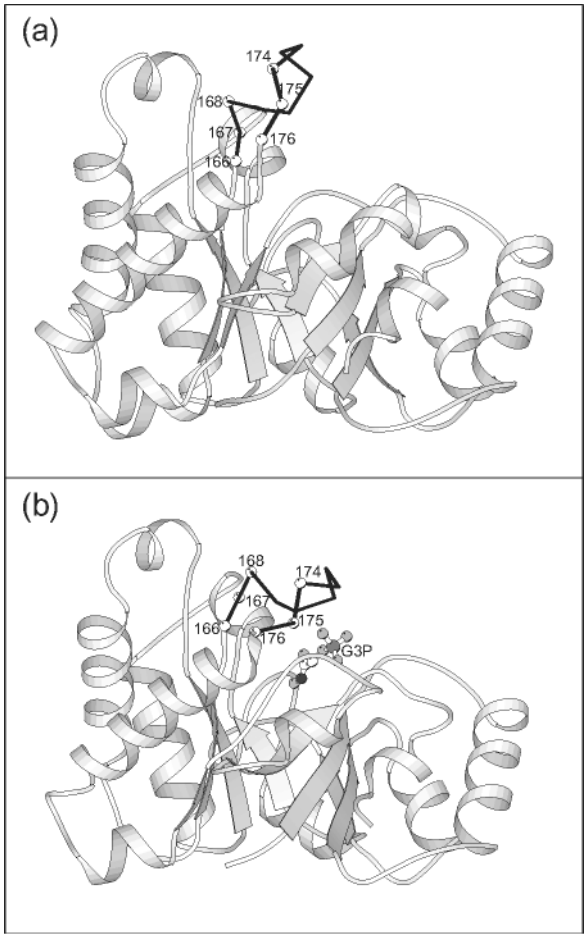

Figure 1. Ribbon diagram of TIM with the loop closed and glycerol 3-phosphate bound in the active site. (a) The open loop.[23] (b) The closed loop with glycerol 3-phosphate (G3P) bound in the active site.[24] The C^{α} atoms of the hinges are represented as balls. This Figure was created with MOLSCRIPT.[25]

Results

The N-terminal hinge library pTMNΛ

A silent restriction site, *Mfe*I, was introduced at the N-terminus of the N-terminal hinge of pTM04[13] for library construction. This vector has a lower expression level of TIM to provide better selectivity in *in vivo* complementation. Before library construction, the plasmid was further modified to prevent wild-type contamination during the construction. A nonsense cassette containing three stop codons (AMB, OPA, and OCH) and an *Nhe*I restriction site was inserted between the *Mfe*I and *Age*I sites to yield pTMNV, the starting plasmid for library construction.

A cassette encoding the N-terminal hinge library was synthesized from oligonucleotides in which each of the three N-terminal hinge codons was replaced with NNS (N: A,T,G, or C, S:G or C). This cassette was inserted between the *Mfe*I and *Age*I sites of pTMNV to produce pTMNΛ, a library of N-terminal hinge mutants of triosephosphate isomerase. Subsequently, this synthesized library was amplified by transformation into DH5α, a non-selective *E. coli* strain. Approximately 200,000 colonies were collected to ensure that more than 95% of all 32,768 possible nucleotide combinations would be included in the library. The accuracy of construction of this library was verified by DNA sequencing and restriction digestion with *Nhe*I. A total of 25 individual colonies were screened. The base-usage observed corresponded to that expected from the synthesized oligonucleotide. After translation, the N-terminal hinge library contained 9261 members from 20 amino acid and amber codon combinations.

The N-terminal hinge mutants

The N-terminal hinge library was selected by *in vivo* complementation of DF502 (tpi) and the enzyme activity screened as described.[13] As shown

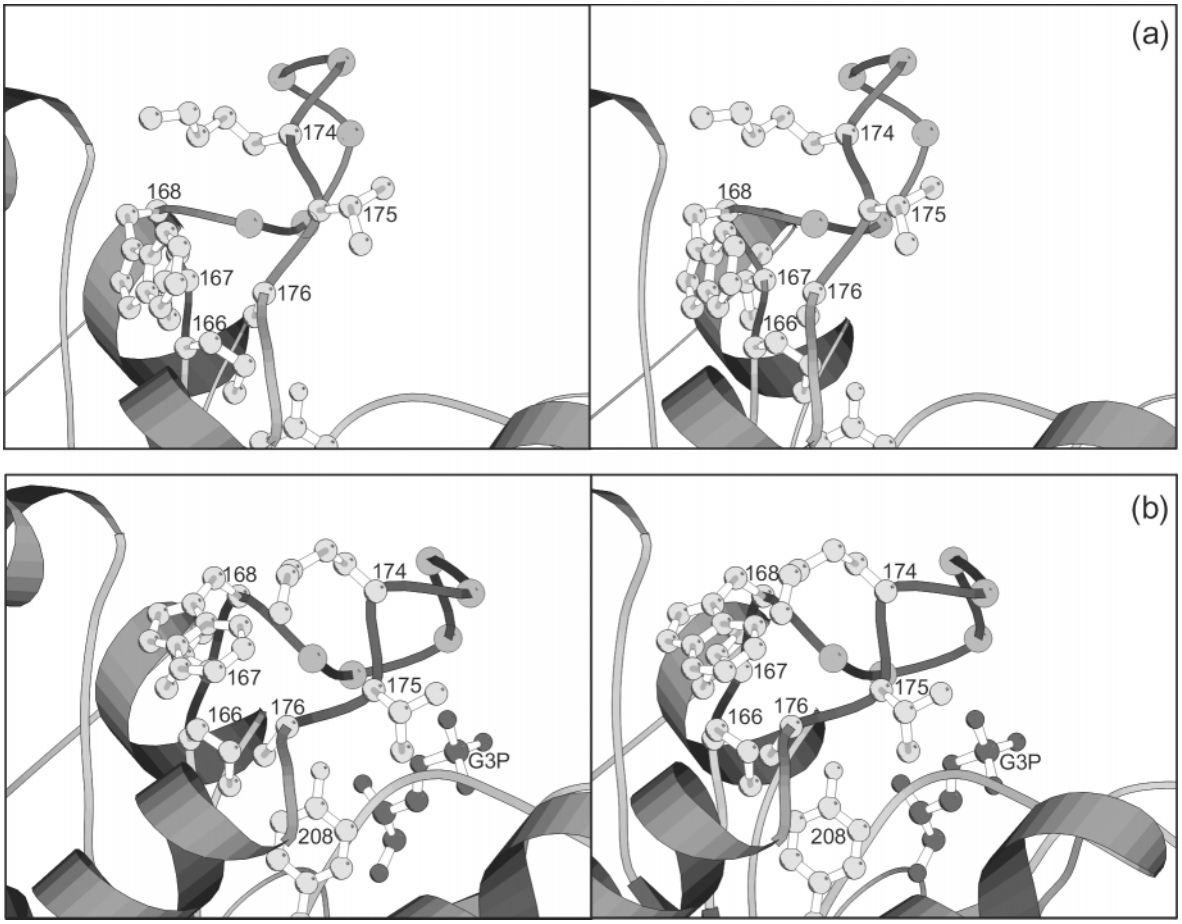

Figure 2. Stereo ribbon diagram of TIM with (a) the loop open and (b) the loop closed and glycerol 3-phosphate (G3P) bound in the active site. The open loop is from the same crystal structure determination as the closed.[23] This Figure was created with MOLSCRIPT.[25]

in Table 1, we sequenced 13 N-terminal hinge mutants that had the largest colony sizes after growth on minimal selective medium. None of the mutants had more than 70 % wild-type activity. In our previous work, we classified 10-70 % of wild-type activity as semi-active. Thus, all 13 N-terminal hinge mutants selected were considered semi-active. To estimate the total number of mutants in the semi-active category, a numerical simulation was performed. Based on the number of mutants selected once and the number of mutants selected twice, we could simulate selection from a pool of mutants using a random number generator. The total number of the semi-active mutants expected is approximately 25. As a result, we have identified about 50 % of the semi-active mutants of N-terminal hinge of TIM.

Interdependence of hinges

To investigate the interdependence of the N-terminal and C-terminal hinges, six active C-terminal hinges representing each previously described family[13] were combined with three semi-active N-terminal hinges, PHS, PTF, and PLH. These three were chosen because they had two amino acid residues that were different from wild-type, and represented a significant change in amino acid side-chain. The specific activities of the 18 ''double-hinge'' mutants are reported in Table 3 and Figure 4. Only five have an activity that is consistent with additive free energy of activation loss of the single mutant parents. The majority of the double-hinge mutants have reduced activity relative to their parent mutants.

Table 1. Sequences of semi-active selected N-terminal hinge mutants

PVY (70)	PIF (40)	PIS (33)	PLW (30)	PLT (24)
PHS (22)	PLH (20)	PIH (20)	PTF (20)	PRW (17)
PFY (16)	PVT (14)	PRS (13)		

Percentage specific activity relative to wild-type TIM is given in parentheses.

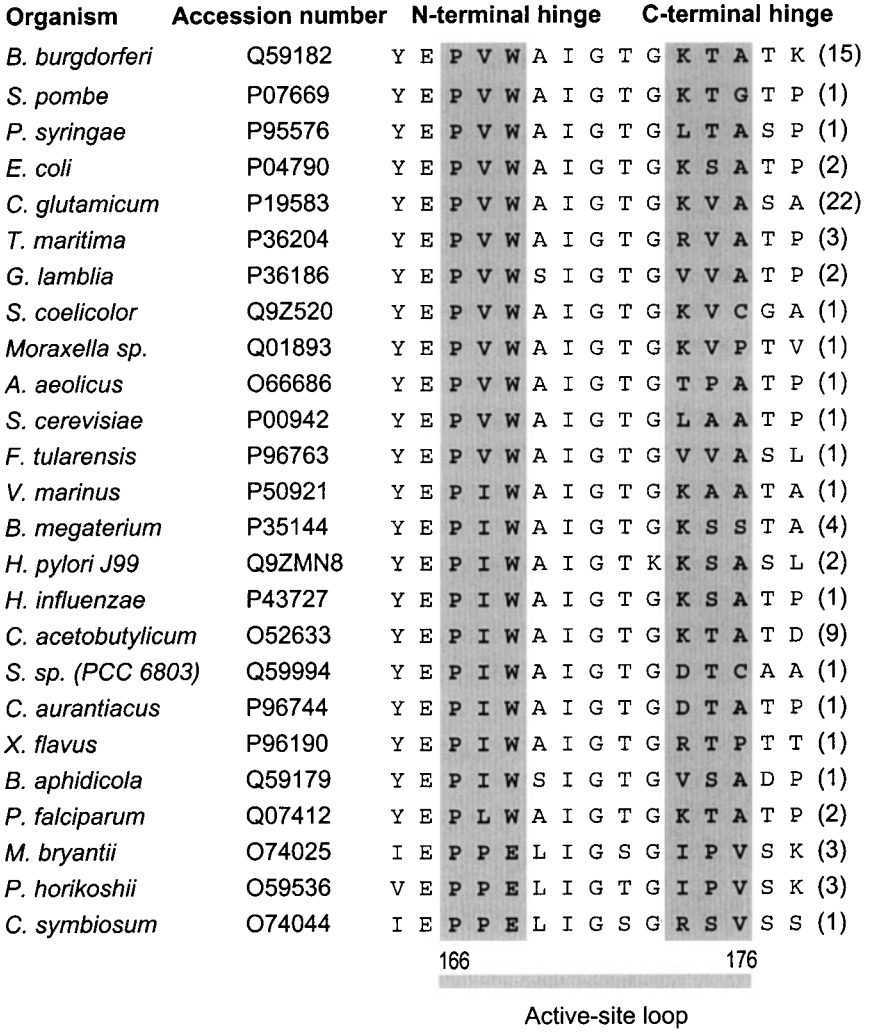

Figure 3. Alignment of amino acid sequences of TIM in the loop region using CLUSTAL W.[26] A representative subset illustrating the variation in loop 6 is presented, because there are 81 known sequences. The number of species containing each loop 6 is indicated in parentheses. The sequences were obtained from the SWISS-PROT data bank.[27]

Loss of enzymatic intermediate

Methylglyoxal and inorganic phosphate are the byproducts that result from decomposition of the enediol intermediate. The rate of inorganic phosphate elimination by the mutants, PHS, PTF, PLH, PHS-KTK, PTF-KTK, and PLH-NPN, is the same as that measured for wild-type, 1.7(±0.2) M^{-1} s^{-1}.

CD spectra and thermal stability measurements

The secondary structure of the mutants was determined using circular dichroism. Spectra were acquired from 190 to 260 nm at 20 °C. All of the mutants appeared to be folded identically with wild-type. Thermal denaturation studies were carried out in the temperature range of 2 °C to 90 °C and monitored at 222 nm. In addition to wild-type, the N-terminal hinge mutants PHS, PTF, and PLF were studied. The melting temperatures (t_m) in the presence of 1 mM 2-PGA were determined at a single protein concentration (1.6 μM; Table 2). This concentration is 10^5 orders of magnitude higher than the estimated K_d (10 pM) for the dimer-monomer equilibrium.[14] Consequently, the measured t_m values were not expected to be dependent on the protein concentration in the range studied. There was no significant change in the cooperativity of the melting curves for each of the mutants investigated (data not shown). All of the mutants and wild-type were irreversibly denatured at 90 °C.

Table 2. The t_m values (°C) of hinge mutants

Mutants	Closed[a]
KTA (WT)	73.6 ± 0.1
PTF	75.2 ± 0.1
PLH	66.5 ± 0.1
PHS	60.1 ± 0.1

[a] Measured from 2 °C to 90 °C at pH 7.6 in the presence of 1 mM 2-PGA.

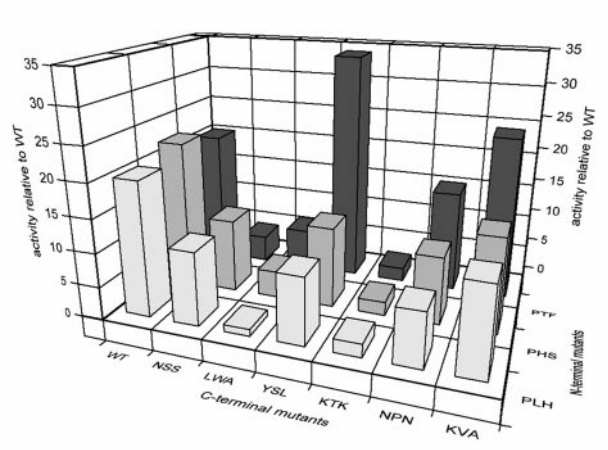

Figure 4. The relative specific activities of double-hinge mutants using GAP as a substrate.

Discussion

TIM is a good model system to study active-site lid function and the importance of hinges for lid motion. TIM catalyzes the interconversion of two simple triosephosphates, GAP and DHAP. There is no cofactor or other substrate. Moreover, TIM is extremely well characterized. The identities and roles of the active-site residues are well established, as are the kinetic methods to study the enzyme. It is known that the active-site lid is critical for binding and positioning the substrate and intermediate.[15] The 11 residue active-site lid is believed to open and close as a rigid body around two hinges that are comprised of three amino acid residues each.[11] We have been investigating the importance of sequence-specific structure in the protein hinge for catalysis.

In previous work, the three residue sequences that function as a C-terminal hinge were determined.[13] We found that five families of sequences worked as hinges. Two families are found in nature, and the other three families represented new sequences. Although these three families were almost as efficient as the native sequences, the rate of formation of the Michaelis complex is slightly slower for these mutants.[16] In this work, we investigated the role of the N-terminal hinge to extend our understanding of the structural requirements for hinges as well as the interdependence of both hinges. The sequences found in nature for the N-terminal hinge are not as varied as for the C-terminal hinge. The N-terminal hinge is not solvent-exposed like the C-terminal hinge, and forms specific hydrogen bonds with the rest of the protein, as well as hydrophobic packing interactions. These interactions could potentially limit the amino acid sequences that might function as a hinge.

The interactions in which the hinges are involved depend on the conformation of the protein, i.e. open *versus* closed. Specifically, the amide oxygen atom of Pro166 forms a hydrogen bond with the amide nitrogen atom of Ala169 in the closed form. An additional hydrogen bond is formed with the amide nitrogen atom of Ile170 in the open form (Figure 5(a)). Hydrophobic packing interactions occur between Pro166 and Trp168, Tyr208, and Tyr164 in the closed form. In the open form, it is residues Trp168, Gly209, and Gly210 that pack with Pro166. The amide nitrogen atom of Val167 is hydrogen bonded to the carbonyl oxygen atom of Glu165, the active-site base, in the open form (Figure 5(b)). This is replaced with a hydrogen bond between Val167 and the carbonyl oxygen atom of Glu129 in the closed form. The amide oxygen atom of Val167 is hydrogen bonded to Ile170 in both conformations. Moreover, Val167 packs with the aliphatic carbon atoms of Glu129 and Ser96 in the open form, and Thr130 in the closed form. Finally, the indole group of Trp168 is hydrogen bonded to the phenol hydroxyl group of Tyr164 in the open form, and with the carboxylate group of Glu129 in the closed form (Figure 5(c)). A hydrogen bond between the amide nitrogen atom of Trp168 and the amide oxygen atom of Glu129 is broken in changing from open to closed. In addition, hydrophobic packing interactions with Arg134, and Thr130 are replaced with van der Waals contacts with Lys174. Contacts with Ala176, Leu131, and Pro166 are maintained in both conformations. Presumably, some of these interactions are formed in the transition state for interconversion of the two species, and their formation affects the rate of interconversion of the species. Molecular dynamics calculations suggest that the hydrogen bonds important for determining the rate of loop closure are those between Ser210 and Gly173, and between Tyr208 and Ala176, whereas the hydrogen

Table 3. Comparison of single and double hinge mutant activities

	C terminus						
N terminus	WT	NSS	LWA	YSL	KTK	NPN	KVA
WT	100	135	108	100	82	79	87
PLH	20	11	1	10	2	8	13
PHS	22	11	4	12	2	10	14
PTF	20	4	6	34	2	15	24

Percentage specific activity relative to wild-type TIM.

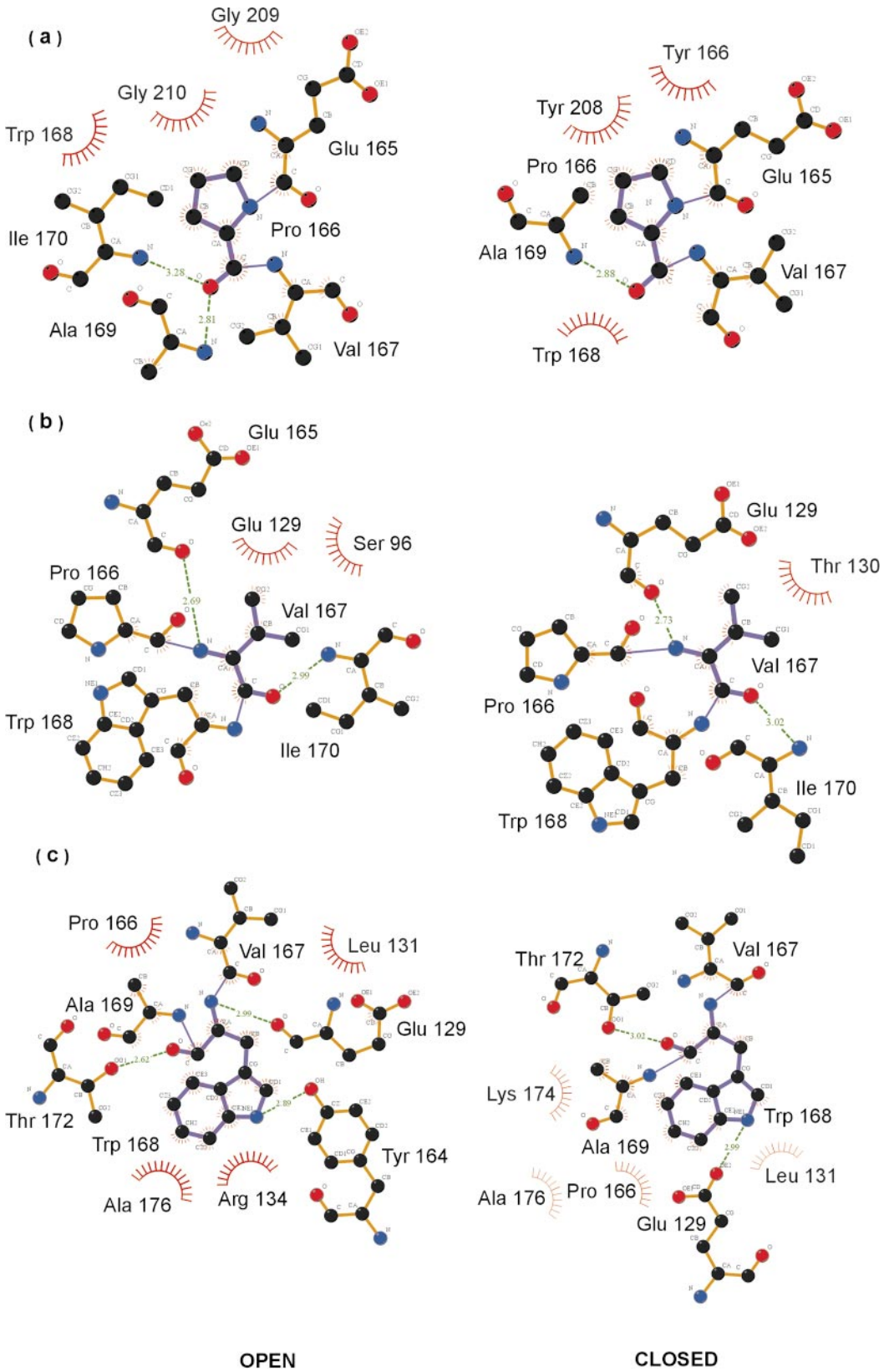

Figure 5. LIGPLOT[28] representation of the interactions of the N-terminal hinge residues with the remainder of the protein in both the open and closed forms. Hydrogen bonds are denoted as broken lines. Residues involved in hydrophobic contacts are represented by a curved comb. (a) Pro166; (b) Val167; (c) Trp168.

bonds formed by residues 166-168 are important for stabilizing the ground state in which they occur.[12] However, these calculations did not examine in detail whether the formation of hydrophobic contacts is important for loop closure.

We explored the relevance of these interactions by constructing an N-terminal hinge combinatorial library. We selected those mutants that could complement DF502, a TIM strain. Thus, we selected mutants that had catalytic activity. We then examined the thermal stability of the closed forms of representative mutants to test the changes in ground-state stability. We monitored methylglyoxal formation as a test for increased rates of loop motion, i.e. alteration of interactions important for closing the loop in a gated fashion. In addition, we constructed and tested double hinge mutants that contained mutant sequences at both the N-terminal and C-terminal hinges. These properties of these mutants provided insight into the importance of hinge-hinge interactions.

Our N-terminal hinge library comprised all possible three residue combinations. All of the mutants selected by *in vivo* complementation of DF502 (tpi) had less than 70 % wild-type (WT) activity. The semi-active (10-70 % WT activity) mutant sequences selected are summarized in Table 1. Amongst all the selected sequences, the most prominent feature is that Pro is strictly conserved at position 166. Although strict conservation would seem to be a basic requirement for TIM activity, because Pro is conserved in wild-type TIM in over 81 species (Figure 3), previous results with the C-terminal hinge library suggested that the absence of a sequence in nature does not preclude its functioning as a hinge. However, Pro166 is adjacent to the active-site base Glu165, which deprotonates the substrate.[17] Closure of the loop positions the Glu for deprotonation. The efficiency of catalysis is dependent on the position of the Glu. For example, mutation of Glu165 to Asp reduces catalytic efficiency and changes the catalytic mechanism.[18] Mutation of Pro166 to any other amino acid removes the above-described packing interactions and could allow the backbone conformation to change, and consequently the position of Glu165 to change.

At position 167, which is Val in chicken TIM, we find that our selected mutants contain Ile, Leu, Thr, His, Phe, and Arg as well as Val. As shown in Table 1, Val, Ile, and Leu are most frequently found and have the highest activities. This is consistent with the prevalence of Val and Ile in this position from many species in nature (Figure 3). The preference for Val, Ile and Leu suggests that van der Waals contacts with Thr130 are important for maintaining the structure of the closed form and, consequently, activity (Figure 5(b)). Although not as ideal, both Arg and Phe provide sufficient hydrophobic surface area for the loop to function at about 10 % of WT efficiency.

At position 168, which is Trp in chicken TIM, we observe conservation of a hydrogen bond donor, e.g. Ser, Thr, His, Tyr, or conservation of the aromatic ring, e.g. Tyr and Phe, in addition to Trp. This suggests that both the hydrogen bond between the Trp indole nitrogen atom and Glu129 as well as packing interactions with Lys174 from the other hinge are important for stabilizing the closed form. The mutants can function, albeit suboptimally, with only the hydrogen bond or the packing interactions.

We chose three mutants, PHS, PLH and PTF, for further study. These mutants represent the most significant changes in side-chain structure. We measured the thermal stability of the closed form of these three mutants using CD spectroscopy to monitor the structure of the protein. The closed form was stabilized relative to the open form by addition of 2-phosphoglycerol, a substrate analog. PTF has the same t_m value as WT; however, the PLH and PHS mutants are less stable. That is, replacement of the second and third hinge residues results in a destabilization of the closed-form ground state and reduced catalytic activity.

We then investigated methylglyoxal production by these mutants. Methylglyoxal is a reaction byproduct that results from elimination of inorganic phosphate from the enediol(ate) phosphate intermediate formed upon deprotonation of GAP or DHAP. It has been demonstrated that the loop, in combination with the binding site, constrains the enediolate intermediate into a planar conformation that disfavors elimination relative to reprotonation and isomerization. In addition, Gly177 of the loop forms a hydrogen bond that holds the intermediate on the enzyme in the closed form. If the enediol intermediate is formed before the loop closes, or if the loop opens before the enediol intermediate is protonated to form product, the enediol intermediate will be released and decompose to methylglyoxal.[15] In other words, if the loop should open too fast relative to the rate of isomerization, methylglyoxal will be formed. Thus, the rate of methylglyoxal formation is viewed as a kinetic measure of loop function and efficiency. The wild-type enzyme is very efficient, forming one molecule of methylglyoxal for every 10^5 molecules of DHAP produced from GAP.[15] In our experiments, we monitored the formation of inorganic phosphate, and thus, indirectly methylglyoxal. The rate of inorganic phosphate elimination by the mutants PHS, PLH and PTF is the same as that of the WT, 1.7 ($\pm$0.2) M ^{1}S ^{1}. This implies that premature release of the intermediate to solution is not the reason why the hinge mutants are less catalytically efficient.

The reduced catalytic activities of these mutants must be due to reduced rates of formation of the Michaelis-Menten complexes or reduced rates of chemical isomerization. The amino acid substitutions selected from our library identify which interactions are important. The mutants isolated have reduced catalytic rates; however, they are the most active mutants present in our N-terminal hinge library. The mutant sequences clearly indi-

cate that hydrophobic packing is very important for efficient formation of the enediol intermediate. However, the reduced catalytic activities are never due to increased rates of loop opening. This suggests that the upper limit on loop rate is not affected by amino acids in the hinge. The upper limit may be determined by the size of the loop and the quantity of solvent that must be displaced in order for it to move 7 Å. However, mutations in the hinge may reduce the rate of loop motion, or may simply slow the rates of substrate and product binding due to steric interference. Solution NMR spectroscopy methods have been developed to measure loop dynamics in the wild-type enzyme directly.[17] These methods will be applied to the hinge mutants in the future to determine whether the mutations slow loop motion or ligand association/dissociation.

In our earlier work, the amino acid sequences that constituted active C-terminal hinges were categorized into five families.[13] To explore the relationship between the N-terminal and C-terminal hinges, three semi-active mutants from the N-terminal hinge selection experiment (PLH, PHS and PTF), and six active C-terminal hinge mutants representing each previously described family were combined (two mutants from one wild-type like family were chosen). By sub-cloning the appropriate fragments, 18 double-hinge mutants were constructed.

Circular dichroism was used to examine the secondary structure of the mutants. Far-UV scans of the mutants are the same as those of WT TIM, implying that there is no major structural perturbation relative to WT. The specific activities were determined (Figure 4, Table 3). Most of the double mutants are less active than expected if the decrease in free energy of activation for each mutant were additive. Only five mutants have activities consistent with additive free energy loss for each mutation. These kinetic results, together with the WT X-ray crystal structure, suggest that the structure of one hinge affects the other. These interactions may be direct; for example, the van der Waals interaction between Trp168 of the N-terminal hinge and Lys174 and Ala176 of the C-terminal hinge. Or the inter-hinge effects may be a result of indirect interference relayed *via* the loop or the main body of the protein. Moreover, the absence of three C-terminal hinge types (represented by YSL, KTK, and NPN) in nature may be due to this interdependence.

To explore if the loop movement is affected by inter-hinge interference, we investigated the methylglyoxal production of selected double mutants as described above. These mutants were chosen for their low activity and non-conservative amino acid substitutions. The rate of inorganic phosphate elimination of the mutants PLH-NPN, PHS-KTK and PTF-KTK was the same as WT, 1.7 ($\pm$0.2) M^{-1} S^{-1}. This implies that the reduced activity of the double mutants is not due to an increased loss of the enediol intermediate.

In summary, only Pro functions in position 166. This is most likely because proper positioning of the active-site base depends on the presence of a proline residue in this position. Moreover, substituting the hinge residues does not result in an increased release of enediol intermediate. However, it appears that specific side-chain interactions are important for forming a catalytically active enzyme. We hypothesize that the hinge side-chains are important for minimizing the number of conformations that may be sampled by the loop during movement. It may be the hydrogen bonds between loop and protein (Gly173-Ser210 and Ala176-Tyr208) and perhaps the intrinsic flexibility of the hinge backbone that are important for maintaining a gated rate of loop closure, not the amino acid side-chains of the hinges. The independence of intermediate release on amino acid sequence is consistent with the absence of a ''universal'' hinge sequence in structurally related enzymes.

Materials and Methods

Reagents

Unless specifically mentioned, all commercial chemicals were used as obtained, and all solvents were dried and distilled by standard methods prior to use. NADH, DL-glyceraldehyde 3-phosphate (diethyl acetal, monobarium salt), and EDTA were purchased from Sigma Chemical Co. (St. Louis, MO). For site-directed mutagenesis, the Quick Change™ site-directed mutagenesis kit from Stratagene (La Jolla, CA) was used following the manufacturer's instructions. For DNA sequencing, the ABI PRISM™ dye terminator cycle sequencing kit with AmpliTaq DNA PolymeraseFS from Perkin Elmer (Foster City, CA) was used according to the manufacturer's instructions. Restriction endonucleases, Klenow fragment of DNA polymerase and phage T4 DNA ligase were from New England Biolabs (Beverly, MA). Alkaline phosphatase was purchased from United States Biochemical (Cleveland, OH). All other reagents were purchased from Fisher Scientific, Inc. (Springfield, NJ).

The buffers used were: buffer A, 100 mM triethanolamine-HCl, 1 mM EDTA (pH 7.9 at 30 °C); buffer B, 10 mM Tris-HCl, 10 mM $MgCl_2$, 1 mM DTT (pH 7.0 at 25 °C); buffer C, 50 mM Tris-HCl, 10 mM $MgCl_2$, 1 mM ATP, 10 mM DTT, 25 μg/mL BSA (pH 7.5 at 25 °C); buffer D, 10 mM Tris-HCl, 1 mM EDTA (pH 7.6 at 25 °C). Luria broth was 10 g of Tryptone, 5 g of yeast extract, and 5 g of NaCl per liter. Minimal medium was M63 salts containing 0.5% (w/v) CAS amino acids, 0.2% (w/v), glycerol, 0.5 mg/l $FeSO_4$, 1 mg/l thiamine, 80 mg/l L-histidine, 100 mg/l streptomycin, and 200 mg/l ampicillin.

Bromohydroxyacetone phosphate (BHAP) was prepared as described.[18] Glycerol-3-phosphate dehydrogenase was obtained from Roche Diagnostics (Indianapolis, IN) and residual TIM activity was removed by treatment with BHAP for one hour, followed by ultrafiltration into buffer A.

Oligonucleotide primers were from Integrated DNA Technologies Inc. (Coralville, CA). The sequences are: **1**, 5′- CCC AAA CTG GCT AAT AGG CAA GAA CC - 3′; **2**, 5′- GGT TCT TGC CTA TTA GCC AGT TTG GG - 3′; **3**, 5′- CCA AAG CAA TTG CTG ATA AC - 3′;

4, 5′- AGT TTT ACC GGT TCC GAT AGC CCA AAC TGG CTA TTA GGC TAG CAC CAC CTT ACT TCA GTC CTT CAC GTT ATC AGC AAT TGC TTT GG - 3′; **5**, 5′- AGT TTT ACC GGT TCC GAT AGC SNN SNN SNN CTC ATA GGC AAG AAC CAC CTT ACT CCA GTC CTT CAC GTT ATC AGC AAT TGC TTT GG -3′.

Bacterial strains

E. coli strains XL1Blue and DH5α were used for plasmid construction. *E. coli* strain DF502 (strep^R, tpi , and his) used for *in vivo* selection was a generous gift from Drs D. Fraenkel and J. R. Knowles, and has been described.[20] The plasmid pBSX1cTIM (wild-type),[21] was a generous gift from Drs E. Komives and J. R. Knowles.

Plasmid construction

pTM05 was constructed by site-directed mutagenesis of pTM04.[13] An *Mfe*I restriction site was introduced at the N terminus of the N-terminal hinge, thus changing codon GCT (Ala) to GCA (Ala). The mutation was introduced by PCR mutagenesis using the Quick Change™ Mutagenesis kit. Primers **1** and **2** were used and restriction digestion and DNA sequencing verified the mutation.

pTMNV was constructed by inserting a cassette containing three stop codons (AMB, OCH, and OPA) and an *Nhe*I restriction site at the N-terminal hinge. A double-stranded DNA cassette was synthesized from primers **3** and **4** that spanned the *Age*I, and *Mfe*I restriction sites. Primer **3** (1.72 μg, 227 pmol) and primer **4** (7.35 μg, 227 pmol) were mixed, denatured at 95 °C for two minutes, cooled to 16 °C over three hours, and treated with Klenow fragment (ten units) in buffer B (40 μl). After polymerization, the cassette was restricted with *Age*I and *Mfe*I, and purified by non-denaturing PAGE (12 % (w/v) acrylamide, TBE buffer). pTM05 (5 μg) was restricted with *Age*I (ten units), and *Mfe*I (ten units) in buffer B, denatured for ten minutes at 70 °C and dephosphorylated for one hour at 37 °C with CIP. The cassette was ligated with the *Age*I-*Mfe*I restricted vector with T4 DNA ligase (400 units) at 16 °C for 16 hours in buffer C. The ligation mixture was transformed into XL1Blue cells. Restriction digestion (*Nhe*I) and DNA sequencing verified the mutation.

pTMNΛ was constructed in a similar fashion by cassette mutagenesis using primers **3** and **5** to synthesize the cassette, Cas-NΛ. Cas-NΛ does not include the *Nhe*I site that is used as a restriction marker in pTMNV. Cas-NΛ was ligated into *Age*I-*Mfe*I restricted pTMNV (5 μg) with T4 DNA ligase (400 units) at 16 °C for 16 hours in buffer B. The ligation mixture was desalted and electroporated into DH5α electrocompetent cells and plated onto LB/Amp agar plates to generate the library. The DH5α colonies on the plate were collected and combined, and the plasmid was purified to yield pTMNΛ, the N-terminal hinge mutant library.

In vivo complementation and screening

In vivo complementation of DF502 on M63 glycerol minimal medium were performed as described.[13]

Specific activity assay of the mutants

The specific activity of the triosephosphate isomerase N-terminal hinge mutants was measured as described.[13]

Combination of hinge mutants

Plasmids encoding NSS, KTK, LWA, NPN, YSL, and KVA at the C-terminal hinge and plasmids encoding PHS, PLH, and PTF at the N-terminal hinge were combined. The 0.8 kb *Age*I to *Eco*RI fragment from each of the C-terminal hinge mutants was subcloned into the 5.5 kb *Age*I to *Eco*RI fragment from each of the N-terminal hinge mutants; thus there are 18 double-hinge mutants. Each mutant was transformed into DF502 and grown on M63 glycerol minimal medium plates for 33 hours at 37 °C. The specific activity of each mutant was determined.

Construction of TIM mutant protein expression plasmids

The 1.3 kb *Pst*I to *Eco*RI fragment from each of the mutants selected from the pTMNΛ library was subcloned into the 2.8 kb *Pst*I to *Eco*RI fragment from pBSX1cTIM (H95N). The *Age*I site in the random cassette region was used as a restriction marker to verify the presence of the hinge mutant.

Protein purification of mutant TIMs

Cell paste (20 g) of DF502(pBSX1c) (PHS, PTF, PLH, and WT) obtained from LB/amp/strep medium (2 l) grown for 24 hours was purified as described.[16]

Methylglyoxal formation

Methylglyoxal formation was monitored at a single substrate concentration using the method of Richard.[22] The enzyme concentration was 30 μM and the [^{32}P]DHAP concentration was 0.15 nM. Time-point samples were collected over 20 hours.

Thermal stability

The CD spectra were recorded on an AVIV 62A circular dichroism spectrometer (Lakewood, NJ) with a 0.2 mm pathlength at 2 °C in the presence of 1 mM 2-PGA. For these experiments, solutions of TIM were equilibrated against buffer D. Protein samples were diluted with the same buffer to a concentration of 40 μM. A baseline spectrum of 1 mM 2-PGA in buffer D was subtracted from the sample spectrum. Temperature denaturation studies were carried out by monitoring the ellipticity at 222 nm as a function of increasing temperature from 2 °C to 90 °C with a scan-rate of 25 deg. C per hour. Cuvettes with a 1 cm path-length were used and the protein concentration was 40 μM. The ellipticity of 1 mM 2-PGA in buffer D was subtracted from the sample ellipticity.

Acknowledgments

This work was supported by a grant from the American Chemical Society, Petroleum Research Foundation (31359G, N.S.). The Center for Analysis and Synthesis of Macromolecules (CASM) at Stony Brook is supported by NIH grant RR02427 and the Center for Biotechnology. Centrifuges and a fluorimeter were purchased with support from the NSF (CHE9808439 and CHE 9709164).

References

1. Kempner, E. S. (1993). Movable lobes and flexible loops in proteins. Structural deformations that control biochemical activity. *FEBS Letters,* **326**, 4-10.
2. Gerstein, M., Lesk, A. M. & Chothia, C. (1994). Structural mechanisms for domain movements in proteins. *Biochemistry,* **33**, 6739-6749.
3. Gerstein, M. & Krebs, W. (1998). A database of macromolecular motions. *Nucl. Acids Res.* **26**, 4280-4290.
4. Rhee, S., Parris, K. D., Hyde, C. C., Ahmed, S. A., Miles, E. W. & Davies, D. R. (1997). Crystal structures of a mutant(βK87T) tryptophan synthase $\alpha_2\beta_2$ complex with ligands bound to the active sites of the α- and β-subunits reveal ligand-induced conformational changes. *Biochemistry,* **36**, 7664-7680.
5. Yang, X.-J. & Miles, E. W. (1992). Threonine 183 and adjacent flexible loop residues in the tryptophan synthase α subunit have critical roles in modulating the enzymatic activities of the β subunit in the α2β2 complex. *J. Biol. Chem.* **267**, 7520-7528.
6. Larson, E. M., Larimer, F. W. & Hartman, F. C. (1995). Mechanistic insights provided by deletion of a flexible loop at the active site of ribulose-1,5-bisphosphate carboxylase/oxygenase. *Biochemistry,* **34**, 4531-4537.
7. Jia, Z., Barford, D., Flint, A. J. & Tonks, N. K. (1995). Structural basis for phosphotyrosine peptide recognition by protein tyrosine phosphatase. *Science,* **268**, 1754-1758.
8. Keng, Y. F., Wu, L. & Zhang, Z. Y. (1999). Probing the function of the conserved tryptophan in the flexible loop of the Yersinia protein-tyrosine phosphatase. *Eur. J. Biochem.* **259**, 809-814.
9. Wang, F., Li, W. Q., Emmett, M. R., Hendrickson, C. L., Marshall, A. G., Zhang, Y. L., Wu, L. & Zhang, Z. Y. (1998). Conformational and dynamic changes of Yersinia protein tyrosine phosphatase induced by ligand binding and active site mutation and revealed by H/D exchange and electrospray ionization Fourier transform ion cyclotron resonance mass spectrometry. *Biochemistry,* **37**, 15289-15299.
10. Karplus, M., Evanseck, J. D., Joseph, D., Bash, P. A. & Field, M. J. (1992). Simulation analysis of triose phosphate isomerase - conformational transition and catalysis. *Chem. Soc. Faraday,* **248**, 239-248.
11. Joseph, D., Petsko, G. A. & Karplus, M. (1990). Anatomy of a conformational change: hinged ''lid'' motion of the triosephosphate isomerase loop. *Science,* **249**, 1425-1428.
12. Derreumaux, P. & Schlick, T. (1998). The loop opening/closing motion of the enzyme triosephosphate isomerase. *Biophys. J.* **74**, 72-81.
13. Sun, J. & Sampson, N. S. (1998). Determination of the amino acid requirements for a protein hinge in triosephosphate isomerase. *Protein Sci.* **7**, 1495-1505.
14. Borchert, T. V., Abagyan, R., Jaenicke, R. & Wierenga, R. K. (1994). Design, creation, and characterization of a stable, monomeric triosephosphate isomerase. *Proc. Natl Acad. Sci. USA,* **91**, 1515-1518.
15. Pompliano, D. L., Peyman, A. & Knowles, J. R. (1990). Stabilization of a reaction intermediate as a catalytic device: definition of the functional role of the flexible loop in triosephosphate isomerase. *Biochemistry,* **29**, 3186-3194.
16. Sun, J. & Sampson, N. S. (1999). Understanding protein lids: kinetic analysis of active hinge mutants in triosephosphate isomerase. *Biochemistry,* **38**, 11474-11481.
17. Rozovsky, S., Jogl, G., Tang, L. & McDermott, A. E. (2001). Solution state NMR investigations of triosephosphate isomerase active site loop motion: ligand release in relation to active site loop dynamics. *J. Mol. Biol.* in the press.
18. de la Mare, C., Coulson, A. F. W., Knowles, J. R., Priddle, J. D. & Offord, R. E. (1972). Active-site labelling of triosephosphate isomerase. *Biochem. J.* **129**, 321-331.
19. Raines, R. T., Sutton, E. L., Straus, D. R., Gilbert, W. & Knowles, J. R. (1986). Reaction energetics of a mutant triosephosphate isomerase in which the active-site glutamate has been changed to aspartate. *Biochemistry,* **25**, 7142-7154.
20. Straus, D. & Gilbert, W. (1985). Chicken triosephosphate isomerase complements an *Escherichia coli* deficiency. *Proc. Natl Acad. Sci. USA,* **82**, 2014-2018.
21. Hermes, J. D., Parekh, S. M., Blacklow, S. C., Köster, H. & Knowles, J. R. (1989). A reliable method for random mutagenesis: the generation of mutant libraries using spiked oligodeoxyribonucleotide primers. *Gene,* **84**, 143-156.
22. Richard, J. P. (1991). Kinetic parameters for the elimination reaction catalyzed by triosephosphate isomerase and an estimation of the reaction's physiological significance. *Biochemistry,* **30**, 4581-4585.
23. Noble, M. E. M., Wierenga, R. K., Lambeir, A.-M., Opperdoes, R. R., Thunnissen, A.-M. W. H., Kalk, K. H., Groendijk, H. & Hol, W. G. J. (1991). The adaptability of the active site of trypanosomal triosephosphate isomerase as observed in the crystal structures of three different complexes. *Proteins: Struct. Funct. Genet.* **10**, 50-69.
24. Zhang, Z., Sugio, S., Komives, E. A., Liu, K. D., Knowles, J. R., Petsko, G. A. & Ringe, D. (1994). Crystal structure of recombinant chicken triosephosphate isomerase-phosphoglycolohydroxamate complex at 1.8-Å resolution. *Biochemistry,* **33**, 2830-2837.
25. Kraulis, P. J. (1991). MOLSCRIPT: a program to produce both detailed and schematic plots of protein structures. *J. Appl. Crystallog.* **24**, 946-950.
26. Thompson, J. D., Higgins, D. G. & Gibson, T. J. (1994). CLUSTAL W: improving the sensitivity of progressive multiple sequence alignment through sequence weighting, position specific gap penalties and weight matrix choice. *Nucl. Acids Res.* **22**, 4673-4680.
27. Bairoch, A. & Boeckmann, B. (1994). The SWISS-PROT protein sequence data bank: current status. *Nucl. Acids Res.* **22**, 3578-3580.
28. Wallace, A. C., Laskowski, R. A. & Thornton, J. M. (1995). LIGPLOT: a program to generate schematic diagrams of protein-ligand interactions. *Protein Eng.* **8**, 127-134.

Edited by P. E. Wright

(Received 21 November 2000; received in revised form 2 February 2001; accepted 5 February 2001)